
NEUROCERIL: ROBOTIC IMITATION LEARNING VIA HIERARCHICAL CAUSE-EFFECT REASONING IN PROGRAMMABLE ATTRACTOR NEURAL NETWORKS

PREPRINT

Gregory P. Davis

Department of Computer Science
University of Maryland
College Park, MD, USA
grpDavis@umd.edu

Garrett E. Katz

Department of Elec. Engr. and Comp. Sci.
Syracuse University
Syracuse, NY, USA
gkatz01@syr.edu

Rodolphe J. Gentili

Department of Kinesiology
University of Maryland
College Park, MD, USA
rodolphe@umd.edu

James A. Reggia

Department of Computer Science
University of Maryland
College Park, MD, USA
reggia@umd.edu

November 15, 2022

ABSTRACT

Imitation learning allows social robots to learn new skills from human teachers without substantial manual programming, but it is difficult for robotic imitation learning systems to generalize demonstrated skills as well as human learners do. Contemporary neurocomputational approaches to imitation learning achieve limited generalization at the cost of data-intensive training, and often produce opaque models that are difficult to understand and debug. In this study, we explore the viability of developing purely-neural controllers for social robots that learn to imitate by reasoning about the underlying intentions of demonstrated behaviors. We present NeuroCERIL, a brain-inspired neurocognitive architecture that uses a novel hypothetico-deductive reasoning procedure to produce generalizable and human-readable explanations for demonstrated behavior. This approach combines bottom-up abductive inference with top-down predictive verification, and captures important aspects of human causal reasoning that are relevant to a broad range of cognitive domains. Our empirical results demonstrate that NeuroCERIL can learn various procedural skills in a simulated robotic imitation learning domain. We also show that its causal reasoning procedure is computationally efficient, and that its memory use is dominated by highly transient short-term memories, much like human working memory. We conclude that NeuroCERIL is a viable neural model of human-like imitation learning that can improve human-robot collaboration and contribute to investigations of the neurocomputational basis of human cognition.

Keywords Imitation learning · Causal reasoning · Programmable neural networks · Cognitive control · Working memory · Symbolic processing

1 Introduction

Humans readily teach and learn using demonstration and imitation. The ability to imitate emerges at an early age and plays a crucial role in early human development, but remains a natural and intuitive method for acquiring new skills throughout the lifespan [1, 2]. Crucially, human-level imitation involves not only replicating observable motor behavior, but also inferring the underlying goals and intentions of the demonstrator. This allows learners to generalize

demonstrated skills to novel environments by abstracting away details that are circumstantial to the demonstration environment.

Programming social robots to carry out complex tasks in a human-like fashion is difficult and typically requires laborious programming by an experienced roboticist. One promising solution to this problem is to develop robots that learn from demonstrations (i.e., robotic imitation learning) [3, 4, 5, 6]. This eases the burden of robotic programming, making it accessible to non-experts. However, most work in robotic imitation learning focuses on reproducing overt motor activity, which affords only limited generalization [3]. Developing more human-like imitation in robots requires algorithms for reasoning about observed actions to construct a deeper understanding of the demonstrator’s goals and intentions that can be adapted to novel environments. This approach also provides a common framework for reasoning about human and robot behavior, which facilitates an understanding of roles and perspectives that promotes seamless human-robot collaboration [7].

Inferring intentions during imitation learning can be viewed as a process of causal reasoning, in which observable behaviors are treated as the effects of hidden causal intentions. Reasoning backwards from effects to possible causes is known as abductive inference, and is a crucial aspect of human diagnostic reasoning and general problem-solving. Algorithms for causal imitation learning may therefore be broadly relevant to cognitive domains beyond overt motor planning, such as language comprehension and visual scene understanding. In addition, insight into the neural basis of these cognitive processes may be gained through the development of robotic imitation learning systems that respect the constraints and neurobiological foundations of human cognition.

In previous work, we developed CERIL, a robotic imitation learning system that uses abductive inference to construct causal interpretations of demonstrated motor behavior and generalizes them for imitation in novel environments [8]. While effective and provably correct, CERIL’s algorithms are implemented with traditional non-neural symbolic programming and have a limited degree of cognitive plausibility. Specifically, CERIL’s inference algorithm involves exhaustive enumeration of plausible causal explanations, which places unrealistic demands on working memory. It also processes demonstrations in an offline fashion, rather than iteratively as humans do.

In this paper, we present NeuroCERIL, a purely-neural imitation learning system that reproduces CERIL’s ability to explain demonstrated behavior during imitation learning. NeuroCERIL is a programmable neural network that implements a novel causal inference algorithm based on the hypothetico-deductive approach, combining bottom-up abductive inference with top-down deductive prediction and verification. Notably, NeuroCERIL processes demonstrations in an online fashion by iteratively constructing efficient data structures in memory that can be used to generate plausible explanations for observed behavior. In other words, NeuroCERIL’s cognitive processes are much more human-like than CERIL’s, and they are supported by neurocomputational mechanisms that more closely resemble those used by people during cause-effect reasoning.

NeuroCERIL’s neural architecture is an extension of NeuroLISP, a neural interpreter for a subset of the Common LISP programming language [9], but includes two major additions: a class system for constructing typed objects with named attributes, and an exception handling system for responding to errors encountered during program evaluation. These innovations show how high-level programming constructs can improve the efficiency and computational capabilities of programmable neural networks, allowing them to learn complex cognitive behaviors.

Our empirical results show that NeuroCERIL is potentially an effective neurocognitive controller for robotic imitation learning systems, as it is able to reproduce CERIL’s performance on a battery of demonstrations of procedural maintenance tasks. We examine NeuroCERIL’s runtime and memory usage during causal inference and show that they scale roughly linearly with the length of the demonstration. Further, many of its memories have very short lifetimes, and are only accessed during a narrow window of processing. Thus, like human working memory, many of its short-term memories are rapidly abandoned, and only a small fraction of its memories need to be maintained through the duration of a demonstration.

2 Related Work

In imitation learning, or learning from demonstration, an agent learns new skills by observing a teacher’s demonstrations. While imitation can be as simple as reproducing motor trajectories, humans are capable of a higher form of imitation that involves reasoning about a teacher’s goals and intentions. This form of imitation, which we refer to as “cognitive-level” imitation, allows learners to grasp the underlying purpose of the demonstrated behaviors and generalize them to novel circumstances. Although its origin remains unclear, cognitive-level imitation emerges in early childhood and plays a crucial role in human cognitive development [10, 1, 11, 12, 13]. Imitation is thought to be supported by neural mechanisms that establish shared representations for perceptually observable behavior and cognitive-motor control processes (i.e., the mirror neuron system), facilitating perspective-taking and interpersonal collaboration [14, 15, 16, 17].

Robotic imitation learning has been proposed as a solution to the complexity and limited accessibility of robotic programming [3, 4, 5, 6]. Despite recent progress, it remains difficult to develop systems that generalize well to novel circumstances and adapt learned behavior to situations that deviate from the demonstration environment. Furthermore, contemporary robotic imitation learning systems often rely on machine learning techniques that require substantial training data and are opaque to users, which makes it difficult to diagnose and debug errors, and creates barriers in trustworthiness and explainability. Safe and effective robotic imitation learning requires human-like algorithms for understanding demonstrated actions, adapting learned skills to novel environments, and constructing explanations of planned behavior that can be understood by end-users.

In previous work, we addressed these challenges by developing CERIL, a robotic imitation learning system based on cause-effect reasoning (Figure 1) [8, 18]. The basic intuition behind this approach is that demonstrated motor behavior is caused by hidden intentions or goals that must be inferred by the learner. To do so, CERIL reasons backwards from effects to plausible causes, a process known as abductive inference, to construct a hierarchy of cause-effect relations that explains the demonstration in terms of high-level intentions. Because these intentions are abstracted from the concrete demonstration, they can be used during imitation to plan a new sequence of motor behavior that implements the learned skill in a novel environment. In addition, CERIL can use these plans to provide explanations for its motor behavior, which allows end-users to investigate and debug its understanding of demonstrated skills. Thus, CERIL uses cause-effect reasoning to understand demonstrated behavior, generalize it to new environments, and explain its own behavior to human users.

CERIL learns from demonstrations that take place in SMILE, a virtual 3D environment with a tabletop and various objects that can be manipulated through manual interactions, such as grasping and moving a block or toggling a switch [19]. Users simulate a sequence of actions demonstrating a skill to be learned, and SMILE records the sequence along with changes in the state of the environment, such as object locations and mutable properties (e.g., the state of a toggle switch). A transcript of the recorded demonstration is then passed to CERIL, which generates an explanation composed of hidden causal intentions that are inferred using a preprogrammed knowledge-base of cause-effect relations.

As noted above, CERIL is effective and provably correct, but its algorithms are implemented with traditional non-neural programming techniques that have a limited degree of cognitive plausibility. To infer intentions, CERIL uses a

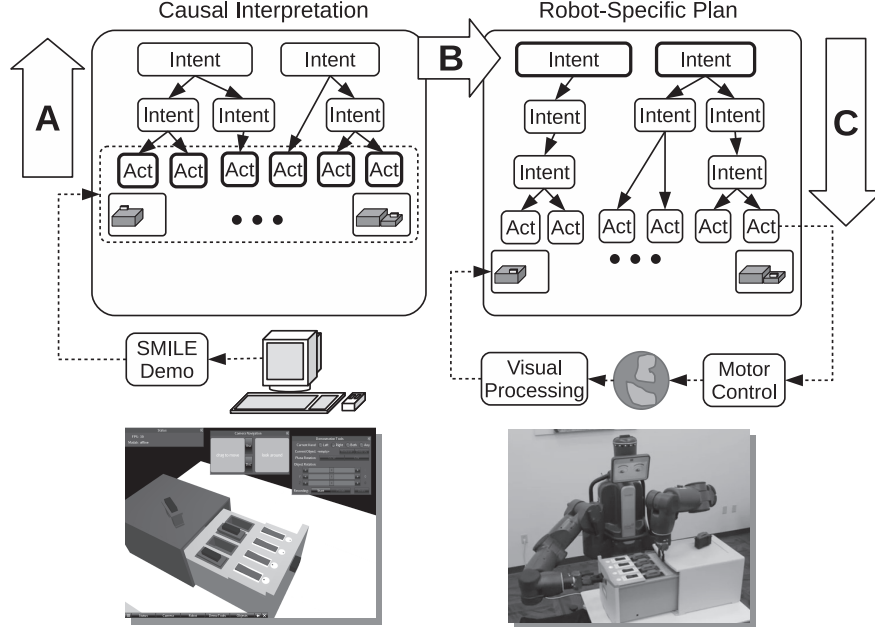


Figure 1: Overview of CERIL’s cause-effect reasoning framework for imitation learning. Demonstrations of a procedural skill are recorded in a virtual environment (SMILE, bottom left) and interpreted to construct a hierarchical causal explanation for observed behavior (left side, A). This explanation is then adapted during imitation to construct a robot-specific plan that implements the learned skill (right side, B and C). CERIL issues low-level motor commands that manipulate objects identified in the environment using visual processing (bottom right). In the present work, we introduce NeuroCERIL, a neurocomputational model that performs the causal interpretation process on the left side of the figure using human-like hypothetico-deductive reasoning. Figure reproduced from [8].

bottom-up dynamic programming algorithm that exhaustively enumerates plausible causal explanations, which places unrealistic demands on working memory. It also requires multiple passes through a demonstration, whereas human imitators reason about demonstrated behavior as it occurs to construct partial explanations before a demonstration is complete. Finally, it is unclear how this approach might be implemented using neural networks to leverage the unique advantages of neural computation, such as its capacity for learning and generalization, and provide insight into the neurobiological foundations of human imitation learning.

Neural approaches to imitation learning typically involve deep neural networks, which require data-intensive training and exhibit a limited degree of generalization in constrained environments [20, 21, 22, 23]. It remains an outstanding challenge to develop neural networks with the high-level cognitive abilities that CERIL exhibits, such as causal inference, compositional modeling, and logical reasoning. Many neural models are incorporated into hybrid systems that delegate these abilities to non-neural algorithms, such as neural-guided search and program synthesis [24, 25, 26]. Furthermore, these models often rely on neurobiologically implausible processes that require simultaneous access to a temporal sequence of inputs or activity states, such as temporal convolutions and attention.

In recent work, we have developed neurocognitive systems that learn to represent and evaluate symbolic programs (i.e., programmable neural networks) [27, 28, 29]. Most recently, we developed NeuroLISP, a programmable neural network with a compositional working memory that can learn to evaluate programs written in LISP, a language with an extensive history in artificial intelligence research [9]. Several features make NeuroLISP an attractive option for modeling human-level cognition in a neurobiologically plausible manner. NeuroLISP can learn to perform high-level cognitive tasks that are difficult for contemporary deep neural networks, such as compositional sequence manipulation, tree traversals, and symbolic pattern matching. Importantly, it learns these tasks using fast associative learning rules that establish robust algorithmic behavior using minimal training data. Its architecture is program-independent, and it represents programs and data using learned attractor states in recurrent neural regions (i.e., distributed representations) that are controlled by top-down gating of both learning and activation. Finally, programmable neural networks can be integrated with neural models of sensorimotor control, including the complex motor control required in robotic imitation learning [30, 31].

In this paper, we explore whether it is viable to develop purely-neural controllers for social robotic systems that behave in a human-like manner. To this end, we develop NeuroCERIL, a programmable neural network that learns human-like algorithms for causal inference during imitation learning (left side of Figure 1). We evaluate our model using CERIL as a target system, as it has been demonstrated to be an effective cognitive controller for bimanual robots. To address CERIL’s limitations in cognitive plausibility, NeuroCERIL implements a novel causal inference algorithm based on the hypothetico-deductive approach, an influential model of diagnostic and scientific reasoning [32, 33, 34, 35, 36]. Hypothetico-deductive reasoning involves a combination of bottom-up abductive inference and top-down predictive verification, which obviates the need for exhaustive search by focusing cognitive processing on relevant causal knowledge. NeuroCERIL therefore serves as a purely-neural controller for social robots that more closely resembles human cognition and learning, facilitates more seamless human-robot interactions, and provides a framework for modeling cognitive processes that are relevant to a broad range of application domains.

3 Methods

NeuroCERIL¹ is a brain-inspired cognitive model that learns procedural skills from demonstrations using cause-effect reasoning. The model’s architecture is an extension of NeuroLISP, a programmable neural network that can store and evaluate programs written in a subset of the Common LISP programming language [9]. NeuroCERIL is programmed with a novel causal inference algorithm based on hypothetico-deductive reasoning, which combines bottom-up abductive inference with top-down deductive prediction and verification. This approach allows NeuroCERIL to anticipate future behavior and focuses cognitive computations on plausible explanations for observed behavior.

Although NeuroCERIL is implemented using attractor neural networks, its distributed neural computations represent algorithmic procedures performed on symbolic data structures. It is therefore convenient to begin by describing its behavior in terms of symbolic information processing. We first outline the robotic imitation learning domain in which NeuroCERIL operates (Section 3.1), and the algorithms and data structures that it uses to implement hypothetico-deductive causal inference (Section 3.2). Then, we present the neurocognitive architecture that learns to represent and evaluate these algorithms and data structures using only neural computations (Section 3.3). Finally, we describe the empirical experiments that we conducted to validate NeuroCERIL, including a battery of test demonstrations that was used to validate CERIL (Section 3.4). We show that NeuroCERIL performs comparably to CERIL, but that its iterative hypothetico-deductive approach is memory efficient and scales well to long demonstrations.

¹<https://github.com/vicariousgreg/neuroceril>

3.1 Robotic Imitation Learning Domain

NeuroCERIL operates in the robotic imitation learning domain designed for CERIL, which involves a bimanual robot (Baxter) learning procedural maintenance tasks [8]. As previously mentioned, a teacher demonstrates these tasks using SMILE, a simulated 3D environment that allows users to interact with virtual objects such as blocks, drawers, switches, and screw valves [19]. SMILE also includes a simulation of the Baxter robot, shown in Figure 2 with a variety of simulated objects. SMILE greatly simplifies the low-level sensory processing involved in recognizing and segmenting actions and objects, allowing us to focus on the higher level cognitive processing that occurs during imitation. When a user is finished recording a demonstration, SMILE produces a transcript containing the sequence of recorded actions, along with a record of changes that occur in the environment, such as changes in object state or location.

Actions are encoded as discrete events with free parameters that refer to objects or locations in the environment. For example, grasping a red-block with the left-gripper is encoded as:

```
grasp<red-block, left-gripper>
```

The identifier `left-gripper` refers to the demonstrator’s left hand, and `red-block` refers to an object in the environment, which is encoded as a collection of named properties:

```
{id:red-block, type:block, color:red, location:loc}
```

Once the block is grasped, its `location` property is updated to `left-gripper` to indicate that it is currently located in the demonstrator’s left hand. This change is represented as a record containing the object identifier, property name, and the new property value:

```
(red-block location left-gripper)
```

Once the block is moved and placed, this property is updated again to reflect its new location. Although locations are encoded as discrete symbols, they can be associated with representations of 3D points in continuous space for use in low-level motor planning.

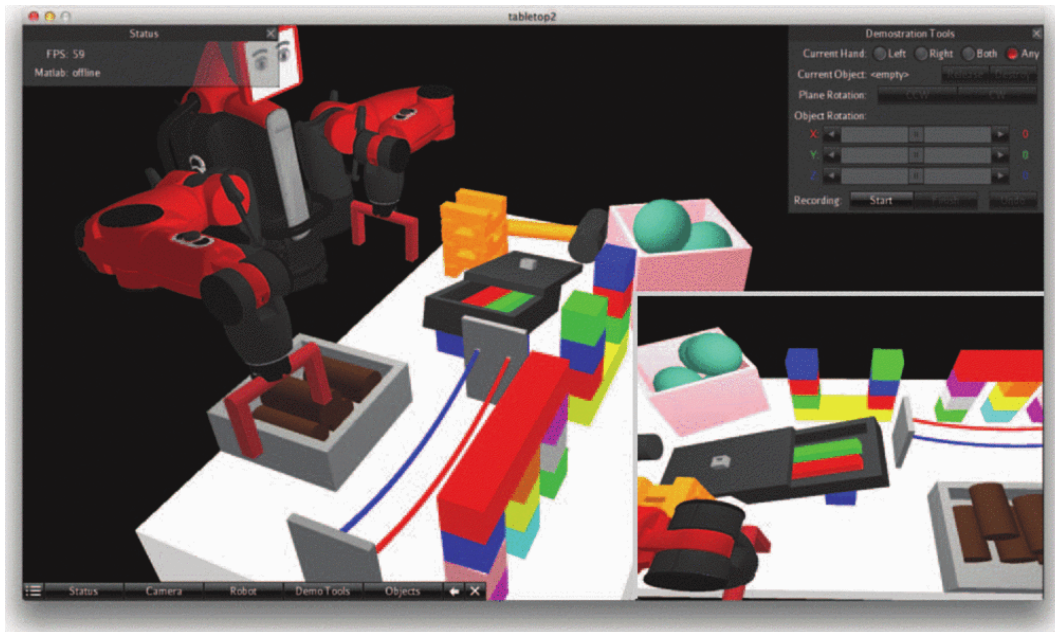


Figure 2: Virtual 3D environment used for recording procedural demonstrations for imitation learning (SMILE: Simulator for Maryland Imitation Learning Environment). The environment contains a tabletop with various objects that can be manipulated, as well as an avatar for a bimanual robot, Baxter (Rethink Robotics). The user can pick up, rotate, move, and release objects on the tabletop to create a sequential demonstration to be used for imitation learning. Figure reproduced from [19].

Like CERIL, NeuroCERIL is pre-programmed with a knowledge-base of cause-effect relations that describe the implementation of abstract intentions. These causal relations are used during learning to infer a demonstrator’s intentions (goals, on left side of arrow) from the demonstrator’s actions (right side of arrow). For example, the intention to `relocate` an object (`obj`) to a target location (`loc`) causes a sequence of concrete motor actions: `grasp` the object, move it to a target location, and `release` the grasp. This is encoded as a template or schema that can be matched to observed behavior:

```
relocate<obj, loc> →
    grasp<obj, gripper>,
    move<gripper, loc>,
    release<gripper>
```

Here, the right arrow represents causation, and indicates that the intention on the left side of the arrow can cause the ordered sequence of actions on the right side. It is important that parameter names (`obj`, `loc`, `gripper`) are repeated in this schema, because this indicates correspondences between the parameters of the intention and the actions that it causes (e.g., the same gripper is used for each action). NeuroCERIL verifies these correspondences when it infers casual intentions in a demonstration. In addition, each schema may include explicit logical predicates that must be satisfied for a cause-effect relation to be plausible. For example, the intention to open a drawer may cause a sequence of grasping, moving, and releasing, but the grasped object must be a drawer handle, and the drawer must be closed prior to opening. These constraints can be encoded as logical statements that NeuroCERIL must verify while inferring causal intentions.

The effects of a causal intention may include other abstract intentions, allowing causes to be chained together to create hierarchies of cause-effect relations. For example, the intention to swap the location of two objects may be implemented as a sequence of `relocate` intentions:

```
swap<obj1, obj2> →
    relocate<obj1, temp>,
    relocate<obj2, loc1>,
    relocate<obj1, loc2>
```

A concrete demonstration of this swapping behavior would involve a sequence of `grasp`, `move`, and `release` actions that are caused by intermediate `relocate` intentions. Thus, inferring the causes of demonstrated actions requires a recursive inference process: when an intention is recognized as a plausible cause, it is treated as the effect of plausible higher-level causal intentions.

NeuroCERIL’s causal knowledge-base may contain multiple schemas describing different implementations of the same intention. For example, the location of two objects may be swapped without placing one in an intermediate location, by instead keeping one object in hand while relocating the other:

```
swap<obj1, obj2> →
    grasp<obj1, gripper>,
    move<gripper, temp>,
    relocate<obj2, loc1>,
    move<gripper, loc2>,
    release<gripper>
```

Here, `temp` refers to a location in the air to which the demonstrator lifts `obj1` to, holding it there while `obj2` is relocated to the original location of `obj1` (`loc1`). A key feature of NeuroCERIL’s knowledge-base is that causal relations are agnostic to the implementation of their effects: a higher-level intention that is implemented using `swap` does not specify which implementation of `swap` to use. This flexibility affords generalization during imitation; a demonstration involving one implementation of `swap` can be imitated using the other implementation. Thus, causal inference allows the imitator to abstract away circumstantial details of the demonstration environment and adapt learned skills to novel circumstances. This may also be necessary if the embodiment of the imitator differs from that of the demonstrator (e.g., number of arms, dexterity, range of motion), requiring the imitator to implement learned skills in a different but equivalent way.

Finally, a sequence of demonstrated actions may have more than one plausible explanation. This may occur if two sequences of cause-effect relations share the same sequence of effects. For example, given the following three cause-effect relations (shown without parameters for simplicity):

```
X → A, B
Y → C
Z → A, B, C
```

a sequence of actions (A, B, C) may be caused by the sequence of intentions (X, Y), or the single intention Z. In this case, the most parsimonious (i.e., simplest or shortest) explanation is usually preferred: (A, B, C) was caused by Z.

In the next subsection, we describe the new hypothetico-deductive causal inference algorithm that NeuroCERIL uses to identify the most parsimonious explanation for a demonstration. NeuroCERIL is provided with a pre-programmed knowledge-base of cause-effect relations with optional logical constraints, as described above. The initial state of the virtual environment is provided as a list of objects encoded as collections of named properties, which may change during the demonstration (e.g., location). The demonstration is encoded as a sequence of parameterized actions, each paired with a list of changes that occur to objects in the environment. The output of this algorithm is a sequence of top-level intentions identified as causes of the demonstrated actions, which serves as an explanation of the demonstration as well as an encoding of the demonstrated skill.

3.2 Hypothetico-Deductive Causal Inference

NeuroCERIL’s approach to causal inference differs from CERIL’s in a way that is more cognitively plausible and memory efficient. Whereas CERIL conducts an exhaustive bottom-up search that makes multiple passes through an entire demonstration, NeuroCERIL uses a more human-like hypothetico-deductive approach that involves a combination of bottom-up and top-down reasoning to iteratively construct a causal explanation for a demonstration as it occurs. When an action is observed, NeuroCERIL consults its cause-effect knowledge-base to generate explicit hypotheses about the demonstrator’s causal intentions (bottom-up), and uses them to deduce testable predictions about subsequent actions (top-down). NeuroCERIL’s cognitive processing is focused on evaluating these predictions to verify or falsify hypotheses. By organizing active hypotheses based on their predictions, NeuroCERIL can efficiently access those that are relevant to an observation, and avoid considering those that are not. When all of the predictions of a hypothesis are verified by observations, the hypothesized causal intention is treated as an observation and processed recursively to identify plausible higher-level intentions that may have caused it. In this way, NeuroCERIL constructs hierarchies of cause-effect relations that are supported by observations, and that represent plausible explanations for sequences of demonstrated behavior. As plausible intentions are identified, NeuroCERIL updates *parsimony pointers* that indicate the shortest sequence of intentions that covers the actions observed so far. At the end of the demonstration, these pointers are traced back to identify the most parsimonious explanation for the entire demonstration. This process is illustrated in Figure 3, outlined as pseudocode in Algorithm 1, and described in more detail below.

NeuroCERIL uses several different data structures to keep track of observed actions, their relative timing, and hypotheses about their causal explanations. These data structures are organized around a timeline, represented in memory as a chain of discrete time-points that delimit observed actions (circles connected by solid arrows in Figure 3). Each action contains pointers to the timepoints immediately before and after it (i.e., start and end points). For concrete primitive actions that are directly observed (e.g., grasping and releasing), these timepoints are adjacent in the timeline (**Action: A** in Figure 3a). However, inferred high-level causal intentions can be implemented with multiple lower-level actions, and can therefore span several timepoints (**Intention: X** in Figure 3c).

Hypotheses originate from a bottom-up abductive reasoning process that we call *evocation*; when an action/intention is observed, NeuroCERIL consults its causal knowledge-base to identify relevant cause-effect schemas that might explain it (top right of Figures 3a and 3c, and first loop of PROCESS_ACTION procedure in Algorithm 1). These schemas are stored in an associative array that maps each action/intention type to a list of schemas that predict it as their first effect. For example, the knowledge-base may contain a schema describing a cause-effect relation between the `relocate` intention and a sequence of `grasp`, `move`, and `release` actions. This schema is stored in the `grasp` list of the knowledge-base, and can be retrieved to evoke a hypothesis that an observed `grasp` action was caused by the intention to `relocate` the grasped object. This hypothesis must be evaluated to determine if the observed action satisfies the constraints of the schema, including correspondences between parameters with shared names as well as explicit logical predicates that must be true for the causal relation to be plausible (VERIFY_HYPOTHESIS procedure in Algorithm 1). Corresponding parameters are matched with a symbolic pattern matching procedure (unification) that we have previously implemented using neural computations [9]. If these constraints are not satisfied, the hypothesis is immediately abandoned. Otherwise, it is added to the timeline and used to make predictions about subsequent actions, as described below. In Figure 3a, the knowledge-base contains two schemas indicating causal relations that might explain the observed action of type A (top right). The evoked hypotheses predict a subsequent action of type B₁ and B₂, respectively (bottom right).

Each timepoint contains a set of hypotheses that make predictions about actions or causal intentions that might occur immediately after it. Like cause-effect schemas in the knowledge-base, these hypotheses are stored in an associative array that maps the predicted action/intention type to the hypotheses that predict it at that timepoint. When an action/intention is observed, the hypothesis set for its starting timepoint is consulted to retrieve the hypotheses that predicted it (second loop of PROCESS_ACTION procedure in Algorithm 1). For the `relocate` example above, the

Algorithm 1 Pseudocode for hypothetico-deductive causal inference algorithm

```

procedure EXPLAIN(demo, init_env)                                ▷ infers causal explanation for demonstration
  curr_env ← init_env                                              ▷ initial environment state
  prev_time ← create timepoint with init_env                      ▷ initial timepoint
  for each action and record of environment changes in demo do
    curr_env ← new environment with changes chained off prior curr_env
    curr_time ← new timepoint with curr_env chained off prev_time
    set action start and end timepoints to prev_time and curr_time
    PROCESS_ACTION(action)
    prev_time ← curr_time
  end for
  return TRACE(curr_time)                                          ▷ reconstruct top-level explanation from timeline
end procedure

procedure PROCESS_ACTION(action)                                ▷ updates timeline and hypotheses
  if action has shorter path to initial timepoint then           ▷ compare with parsimony pointer
    update parsimony pointer for action's end timepoint
  end if
  for each schema predicting action type as first effect do      ▷ new hypotheses
    hypothesis ← generate hypothesis from schema                 ▷ abductive evocation
    VERIFY_HYPOTHESIS(hypothesis, action)
  end for
  for each hypothesis predicting action type at action end timepoint do ▷ old hypotheses
    VERIFY_HYPOTHESIS(hypothesis, action)
  end for
end procedure

procedure VERIFY_HYPOTHESIS(hypothesis, action)                ▷ verifies a hypothesis for cause of action
  if action matches hypothesis prediction then                ▷ unification and constraint checking
    if hypothesis is fully matched then                        ▷ all predictions verified
      intent ← generate causal intention from hypothesis
      PROCESS_ACTION(intent)                                    ▷ process inferred intention as an observed action
    else
      update hypothesis prediction
      add hypothesis to action's end timepoint                  ▷ advance hypothesis in timeline
    end if
  end if
end procedure

procedure TRACE(curr_time)                                       ▷ traces top-level explanation using parsimony pointers
  intent ← parsimony pointer of curr_time
  prev_time ← start timepoint of intent
  if prev_time is initial timepoint then
    return list containing intent                                ▷ first intention in top-level sequence
  else
    prior_intents ← TRACE(prev_time)                            ▷ recursion
    append intents to prior_intents
    return prior_intents
  end if
end procedure

```

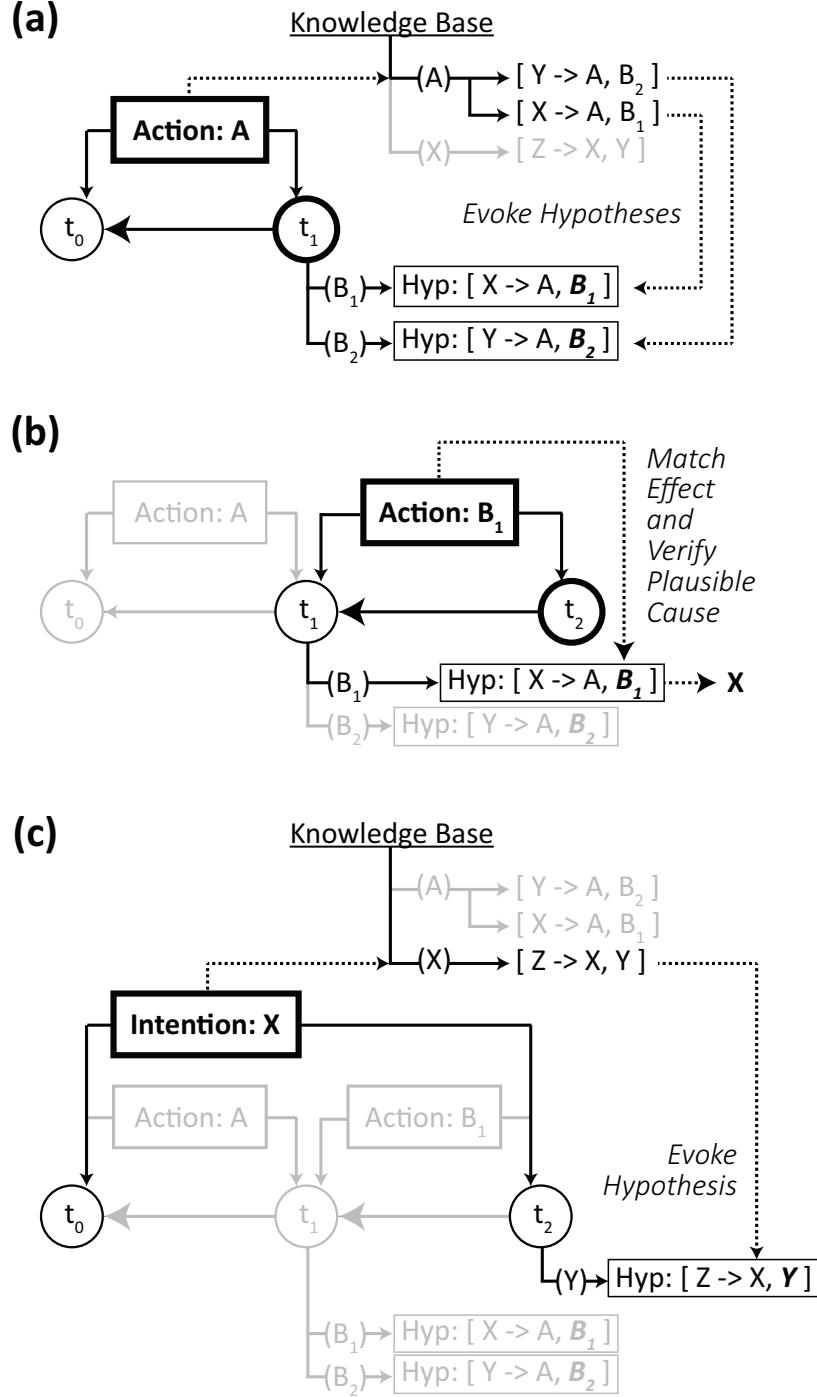


Figure 3: Hypothetico-deductive process for inferring hierarchical intentions during imitation learning. **(a)** An action of type A is observed at timepoint t_1 and added to a chain of timepoints in memory (bold box and circles, left). The knowledge base (top right) is consulted to evoke plausible hypotheses about the action's cause. These hypotheses are added to timepoint t_1 (bottom right) and stored according to their subsequent predictions (B_1 and B_2). **(b)** An action of type B_1 is observed at t_2 (center), and matched to the hypothesis that predicted it, generating a plausible causal intention of type X (bottom right). **(c)** This intention is processed recursively as an observation spanning t_0 to t_2 (left). A hypothesis is evoked that predicts an intention of type Y at t_2 (bottom right).

evoked hypothesis predicts that the demonstrator will move the grasping arm immediately after the grasp action occurred. When move is observed, this hypothesis is retrieved and evaluated to determine if its prediction was satisfied. This involves verifying the schema’s logical constraints, as described above. If these constraints are satisfied and the hypothesis predicts further actions, the next prediction is retrieved, and the hypothesis is advanced to the next timepoint. When all of the predictions for a hypothesis are verified, it is used to generate a plausible causal intention that is added to the timeline. This intention is then processed recursively in order to generate and verify further hypotheses about its underlying cause (call to `PROCESS_ACTION` procedure within `VERIFY_HYPOTHESIS` procedure of Algorithm 1). In Figure 3b, the observed action of type B_1 matches the prediction of a hypothesis at t_1 , and the corresponding causal intention of type X is generated (bottom right). This intention is then processed as an observation in Figure 3c, and a new hypothesis is evoked proposing that an intention of type Z is the underlying cause. This new hypothesis predicts an intention of type Y at time t_2 , and is added to the timeline accordingly (bottom right).

Each timepoint also contains a representation of the state of the environment that is consulted during hypothesis verification (Figure 4). The environment contains several objects with named properties that can change over the course of a demonstration. At the beginning of the demonstration, NeuroCERIL is provided with a full specification of the initial state of the environment. When an action is observed, NeuroCERIL is also provided with a list of changes to object properties that were caused by the action. Rather than maintaining full copies of the environment state at each timepoint, which would require substantial memory, NeuroCERIL stores a record of these changes that can be consulted to determine the state of the environment at a given timepoint (or its initial value if it was not changed). To query the state of an object property at a given timepoint, NeuroCERIL retrieves the most recent change that occurred to that property prior to that timepoint. To support this operation, each timepoint stores a nested associative array, where the outer array stores entries for changed objects, and each inner array stores entries for a particular object’s changed properties. Importantly, the inner arrays representing changes to the same object at different timepoints are chained together (dotted lines in Figure 4).

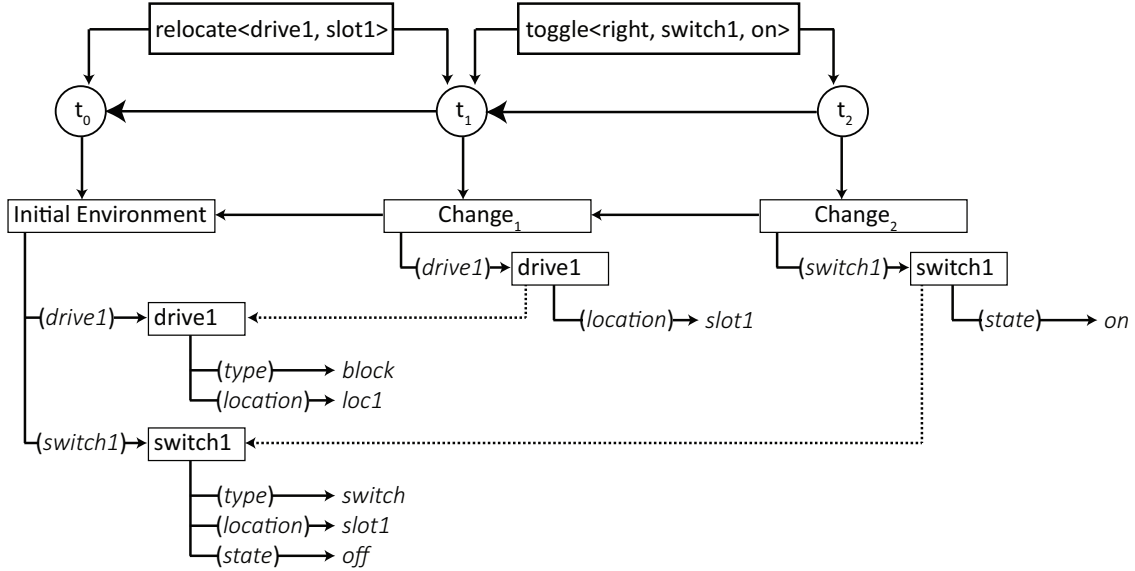


Figure 4: Representing a changing environment in memory during a simple demonstration, in which a hard drive (*drive1*) is moved from an initial location (*loc1*) to a slot (*slot1*), and an adjacent switch (*switch1*) is toggled *on* with the *right* hand. Each action is stored in a timeline of discrete timepoints (circles connected by solid arrows, top; see Figure 3). The initial timepoint (t_0 , top left) stores a representation of the initial environment as a nested associative array (“Initial Environment”, left). Each entry in the array maps a symbolic name to an object (*drive1* or *switch1*, bottom left). Objects are stored as inner associative arrays, which map symbolic names of properties to their corresponding values (e.g., the *location* of *drive1* is initially *loc1*). Subsequent timesteps store records of changes that occur in the environment (“Change₁” and “Change₂”, center and right). Like timepoints, these records are chained together in reverse chronological order, and each record is stored like the initial environment as a nested associative array. The inner associative arrays of corresponding objects are also chained together (dotted lines). This compact representation uses minimal memory, but affords access to the state of the environment at each timepoint.

Finally, NeuroCERIL maintains pointers in memory that can be used to retrieve the most parsimonious explanation for the actions observed so far. The best explanation is the shortest sequence of intentions that covers all directly observed primitive actions without gaps or overlaps. This is represented by a chain of alternating timepoints and intentions that leads from the last timepoint to the first timepoint. Thus, each timepoint maintains a *parsimony pointer* to the intention that provides the shortest path back to the first timepoint in the demonstration. Whenever a plausible intention is identified, it is compared with the current best intention for the intention’s end timepoint (beginning of `PROCESS_ACTION` procedure in Algorithm 1). NeuroCERIL performs this comparison by iterating through the paths simultaneously until the initial timepoint is reached. If the newly identified intention provides a shorter path to the initial timepoint, it is replaced as the current best intention for the end timepoint. When the demonstration is complete, the best explanation for the full sequence of observed actions can be reconstructed by following the chain of parsimony pointers from the final timepoint back to the initial timepoint (`TRACE` procedure in Algorithm 1).

3.3 Neural Implementation

NeuroCERIL’s architecture (shown in Figure 5) is an extension of NeuroLISP, a programmable neural network that learns to store and evaluate programs written in a subset of the Common LISP programming language. Many of the details of NeuroCERIL’s functionality are shared with NeuroLISP and can be found in [9]. Here we provide a brief overview and highlight the novel features of NeuroCERIL’s architecture that extend its computational capabilities beyond NeuroLISP.

Like NeuroLISP, NeuroCERIL represents programs and other symbolic data structures as learned systems of dynamical attractor states and associative transitions between attractor states [27]. Programs are evaluated via top-down control of gated connectivity between and within neural regions. This guides the flow of activity according to instructions retrieved from neural memory, much like a conventional computer architecture controls data flow according to instruction opcodes. Importantly, NeuroCERIL also controls its own learning in this way, allowing it to construct, access, and modify data structures stored in memory during program evaluation. Inputs and outputs are mediated by gated connectivity between the outer environment and a special region that represents discrete symbols as unique patterns of activity (`lex`, center of Figure 5). These connections allow NeuroCERIL to read symbolic inputs, including representations of programs, and output the results of program evaluation. During imitation learning, a demonstration recorded in SMILE is provided as a sequence of symbolic inputs, and NeuroCERIL outputs a sequence of symbolic outputs that encodes the inferred causal explanation.

NeuroCERIL is initialized with a learned program-independent virtual machine composed of procedures that implement the primitive operations of its programming language [28]. After initialization, NeuroCERIL is programmed with the causal inference algorithm described in Section 3.2, which is expressed in the language of NeuroCERIL’s virtual machine. The details of initialization and program learning can be found in [9].

NeuroCERIL’s virtual machine supports two major innovations that extend its computational capabilities beyond NeuroLISP and ease the implementation of its causal inference algorithm: a class system and an exception handling system. The class system allows specification of reusable programs (i.e., class methods) for initializing and modifying instances of complex data structures such as causal hypotheses, cause-effect knowledge, and observed actions. Instances of classes, called objects, are stored as collections of named pointers to other memories (i.e., class attributes). The underlying implementation of objects makes use of the existing mechanisms for variable binding in NeuroCERIL’s virtual machine; objects have corresponding lexical namespaces that store attributes as variable bindings (see [9] for details on variable binding in NeuroLISP).

Exceptions are errors that occur during program evaluation, and are triggered by events such as attempted access to undefined variables, attributes, or class methods. The exception handling system provides a mechanism for specifying dynamic responses to exceptions. This obviates the need for excessive program expressions that perform checks on data before access; a program instead can specify what should be done if retrieval fails. For example, when evoking hypotheses to explain an observed action, NeuroCERIL consults its causal knowledge-base to retrieve cause-effect recipes that are relevant to the observed action (see Section 3.2). If the knowledge-base does not contain any entry for the observed action type, retrieval will result in an exception that can be easily handled by skipping the evocation process.

Exception handling is supported by the `exception stack` region (bottom right of Figure 5), which maintains pointers to activity states in other regions that represent the state of the virtual machine. This region functions like the `runtime` and `data stack` regions (shared with NeuroLISP), which represent stack frames as distributed patterns of activity that have learned associations with activity patterns in other regions [9]. Responses to exceptions are specified in programs with “try” expressions that include a primary sub-expression to evaluate, and an additional sub-expression representing the response. When a “try” expression is evaluated, the virtual machine first stashes its state on the exception stack,

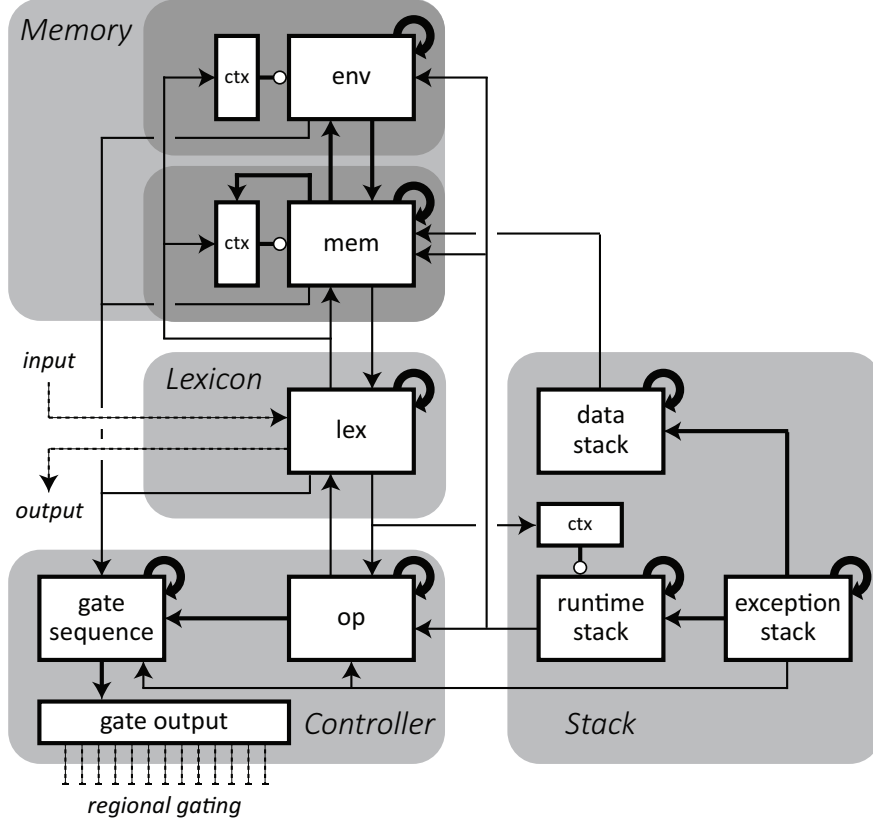


Figure 5: NeuroCERIL’s neurocognitive architecture that learns to perform hypothetico-deductive causal inference. This architecture is an extension of NeuroLISP [9], and is made up of several recurrent neural regions (boxes) with inter-regional connections (solid arrows) that are divided into sub-networks (grey background boxes). Like NeuroLISP, NeuroCERIL implements an interpreter for a LISP-like programming language that is used to implement high-level algorithms. Programs and other data are stored as systems of learned attractors in the *mem* region (center), and are evaluated via top-down control of connection gates (*regional gating*, bottom left). Inputs and outputs to the model are mediated by the *lex* region (center), which represents symbols as distributed patterns of activity that can be dynamically associated with activity patterns in adjacent regions (e.g., data structures in *mem*). NeuroCERIL implements a new class system using existing circuitry for variable bindings (connectivity between the *mem* and *env* regions, top), and also includes a new *exception stack* region (bottom right) that supports exception handling. These new features allow for efficient implementation of the causal inference algorithms described in this paper (see text for details).

which involves learning associations in the pathways exiting the *exception stack* region. Then, the virtual machine attempts to evaluate the primary sub-expression. If an exception occurs, the virtual machine retrieves its prior state from the *exception stack*, and evaluates the response sub-expression. Upon completion, the top of the *exception stack* is popped, and evaluation of the program continues.

3.4 Experimental Evaluation

To evaluate NeuroCERIL, we performed empirical experiments using a battery of test demonstrations that was used to test CERIL. These tests include procedural maintenance tasks involving replacing, swapping, and discarding mock hard drives in a docking assembly, as well as toy block stacking tasks (see [8] for details). We compared NeuroCERIL’s output with CERIL’s to confirm that it performs comparably, and carried out additional analysis on its memory usage and runtime to determine how well it scales with the length of demonstrations.

Runtime was measured as the number of timesteps in model simulations, and memory usage was evaluated by monitoring each simulation to count the number of associations that were learned during causal inference. Specifically, we monitored learning of attractor states and transitions in the underlying neural networks (stored in the recurrent connectivity of the *mem* region in Figure 5), as well as associations between namespaces and memory states that represent

variable bindings for both local variables and object attributes (stored in the connection from *env* to *mem* in Figure 5). These associations represent the core data structures used during causal inference, such as observed actions, hypotheses, and inferred causes. We report the associations formed specifically during the inference process, and exclude those that represent the causal inference programs and cause-effect knowledge that is shared across demonstrations.

We further examined NeuroCERIL’s memory access patterns to gain a better understanding of its memory usage. We hypothesized that the majority of memories constructed during inference would be highly transient memories that are only accessed across brief intervals of time, such as abandoned causal hypotheses. This would indicate that NeuroCERIL might benefit from a functionally distinct short-term memory system in which memories rapidly fade if they are not refreshed by retrieval, much like human working memory. To test this hypothesis, we recorded instances of memory construction and access during inference, excluding demonstration-independent memories such as program representations and cause-effect knowledge. For each recorded memory, we determined its “lifespan” as the interval between its initial learning and the final time it was retrieved during the simulation (i.e., a memory is “born” when it is first learned, and “dies” after its last retrieval during the simulation). We then calculated the number of “living” memories over the course of the inference process and compared it to the total number of memories constructed. This provides a metric for the proportion of memories that are being actively utilized for causal inference.

4 Results

Table 1 shows the results for the same benchmark battery of procedural maintenance task demonstrations that were used to verify CERIL’s functionality. For each task, we report the number of actions recorded in the demonstration (**Act**), the number of top-level intentions in NeuroCERIL’s causal interpretation (**Interp**), the number of timesteps of neural network simulation required for causal inference (**Timesteps**), and three measurements of learned associations that indicate model memory usage: the number of learned attractors (**Attr**) and attractor transitions (**Transit**) in the *mem* region, and the number of learned variable bindings (**Bindings**). NeuroCERIL produced causal interpretations (sequences of top-level intentions) equivalent to the minimum cardinality explanations identified by CERIL for each of the tests. Figure 6 shows an example of the causal interpretation inferred for the *replace red with spare (1)* task.

Table 1: NeuroCERIL performance on battery of robotic imitation learning tasks

Demonstrated Task	Act	Interp	Timesteps	Attr	Transit	Bindings
Remove red drive (1)	7	3	353825	197	362	661
Remove red drive (2)	10	4	490085	250	468	917
Replace red with spare (1)	14	6	653758	341	642	1243
Replace red with spare (2)	14	6	653758	341	642	1243
Replace red with green (1)	15	7	668955	356	670	1276
Replace red with green (2)	15	7	668955	356	670	1276
Swap red with green (1)	16	8	668889	357	672	1278
Swap red with green (2)	16	8	668981	361	680	1285
Toy blocks (IL)	24	8	1224377	591	1150	2326
Toy blocks (AI)	30	10	1524253	735	1434	2905
Toy blocks (UM)	39	13	1975927	945	1848	3763

Runtime and memory usage results provide an empirical estimate of the complexity of NeuroCERIL’s hypothetico-deductive causal inference algorithm. Figure 7 shows runtime and memory usage relative to the length of input demonstrations (**Act** in Table 1). Each datapoint corresponds to a row in Table 1, and the dashed lines show the results of linear regression computed for each metric. These results can be compared to Table 1 in [8]², as well as the theoretical analysis of CERIL’s complexity. Whereas CERIL exhibits a super-linear scaling of runtime and memory usage (indicated by the number of recognized top-level covers), NeuroCERIL’s runtime and memory usage scale linearly with the length of the demonstration. This is due to its online processing of demonstrations and incremental updating of data structures in memory that implicitly represent possible explanations.

In further analysis of memory usage, we focus on learned memory attractors, as they are a bottleneck for neural attractor memory [27]. We present the results for the *replace red with spare (1)* demonstration, but note that the results for other demonstrations are comparable. Figure 8a shows the “lifespans” of memory attractors constructed during causal inference for this demonstration, computed as the interval between initial learning and final retrieval. The x-axis indexes

²We used slightly more complex versions of the IL and AI block stacking tasks that include more blocks and actions than those reported in [8].

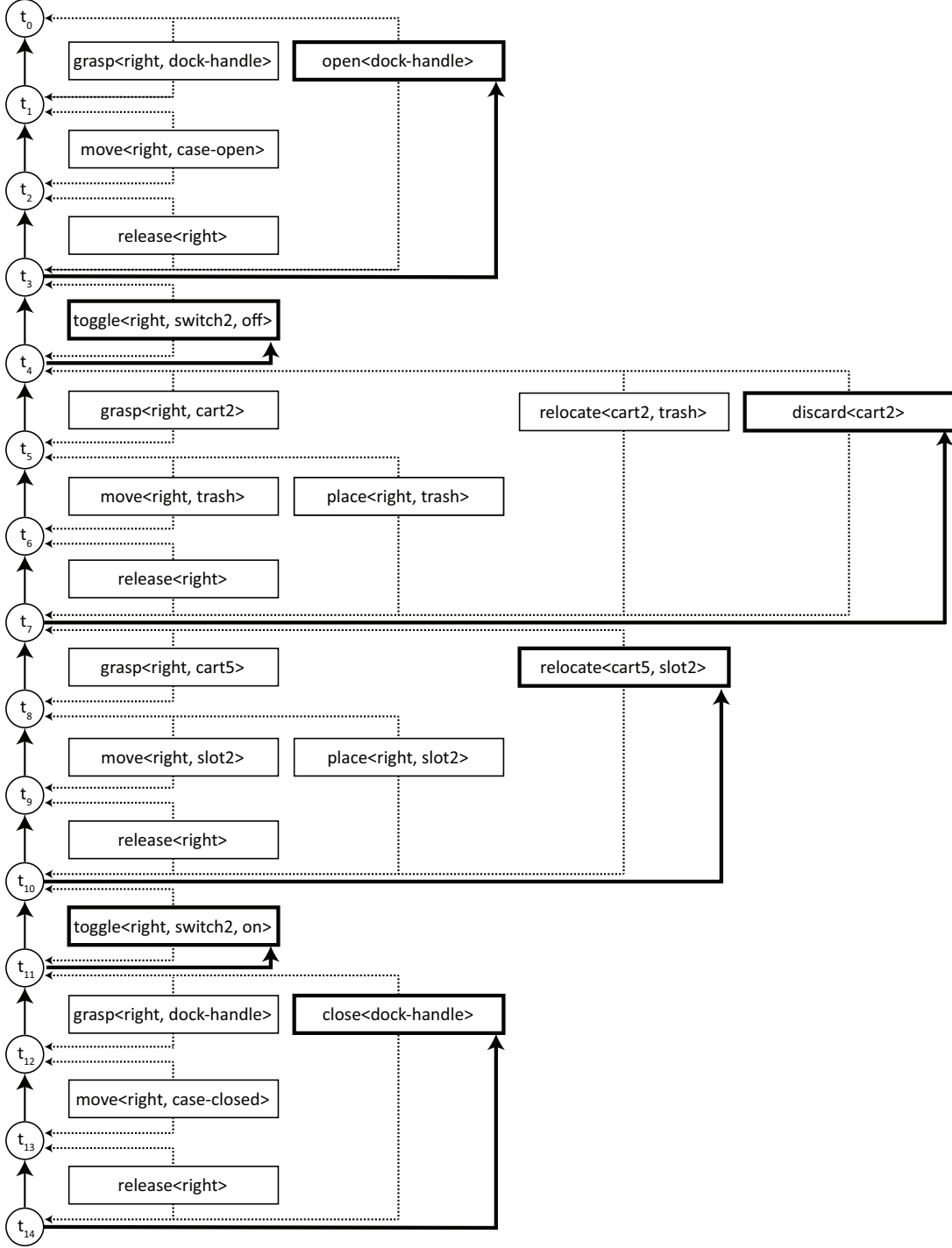


Figure 6: Causal interpretation produced by NeuroCERIL for the *replace red with spare (1)* task, which involves replacing a broken disk cartridge (*cart2*) in a mock disk drive drawer with a fresh cartridge (*cart5*). Actions and causal intentions are represented by rectangles that indicate the type of action/intention along with its parameters. Each action/intention points to its start and end timepoints, represented by circles (left side), which delineate concrete observed actions (leftmost column of boxes). The top-level explanation, composed mostly of abstract intentions, is indicated by bold boxes. NeuroCERIL reconstructs this explanation by following the shortest path from the final (t_{14}) to initial (t_0) timepoints using parsimony pointers (bold arrows, shown only for relevant timepoints; see Section 3.2).

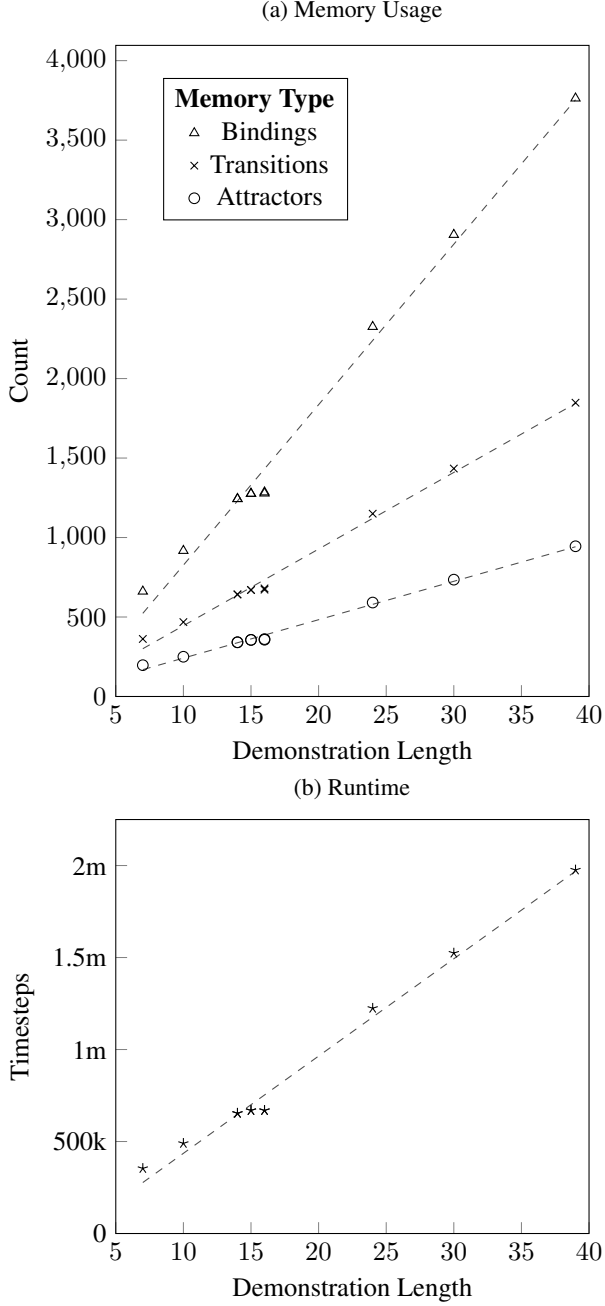


Figure 7: NeuroCERIL’s memory usage and runtime during causal inference. Each data point corresponds to an individual imitation learning test task (rows in Table 1). Dashed lines are lines of best fit computed with linear regression, and show that memory usage and runtime scale linearly with the length of the demonstration (x-axis). **(a)** Memory usage is reported as the number of learned attractor states, attractor transitions, and variable bindings generated during causal inference (see text for details). **(b)** Runtime is reported as the number of timesteps of neural model simulation required for causal inference.

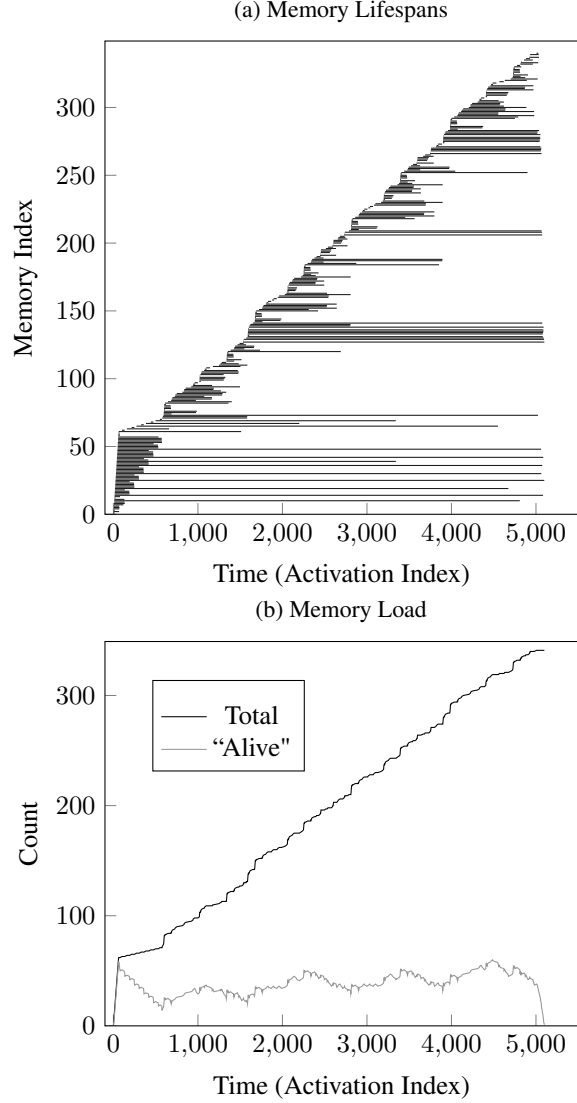


Figure 8: “Lifespans” of memory attractors constructed during causal inference on the *replace red with spare (I)* task, reported as the interval between initial learning and final retrieval. The x-axis indexes model simulation timesteps in which an attractor is learned or retrieved. **(a)** Each horizontal line represents the lifespan of one memory attractor, indexed along the y-axis. Shorter lines indicate that a memory attractor is only accessed over a brief interval, while longer lines indicate memories that are utilized over longer periods of time. **(b)** Memory load, reported as the total number of memories learned over time compared to the number of “living” memory attractors (i.e., attractors that have been learned at or before a given time and will be retrieved at a later time). While the total number of memories steadily increases over time, the majority of these memories are rapidly abandoned, and are only accessed over a brief period of time.

timesteps in which a memory attractor is constructed or retrieved, and each horizontal line indicates the lifespan of one memory attractor, indexed along the y-axis. Some memories remain alive through the majority of the inference process, such as representations of the environment and inferred causes that make up the final top-level cover. Others have relatively short lifespans, such as falsified causal hypotheses. We refer to the “living memories” at a given timestep as the set of memories that have been learned prior to that timestep, and that will be accessed at a later timestep (i.e., a memory “dies” after the final timestep in which it is accessed). Figure 8b shows the total number of memory attractors learned over the course of the inference process, along with the number of “living” memories at each timestep, which corresponds to the number of overlapping horizontal lines at each point along the x-axis in Figure 8a. Although the total number of learned memories increases steadily over time, the majority of these memories have relatively short lifespans. As a result, the number of “living” memories remains fairly stable over time, and never exceeds 20% of the total learned memories.

5 Discussion

In this paper, we presented NeuroCERIL, a brain-inspired neurocognitive controller for social robots that learn procedural tasks from human-provided demonstrations (i.e., robotic imitation learning). NeuroCERIL infers the intentions underlying demonstrated behavior using a novel causal inference algorithm based on human-like hypothetico-deductive reasoning, which combines bottom-up abductive inference with top-down predictive verification. This approach allows NeuroCERIL to iteratively construct plausible interpretations of demonstrated behavior as it is observed, make verifiable predictions about subsequent behavior, and generate compact explanations in terms of abstract intentions that can be generalized to novel environments. We evaluated NeuroCERIL on a benchmark battery of procedural maintenance and toy block-stacking tasks recorded in a virtual environment, demonstrating that it works effectively in robotic imitation learning domains. Our empirical results also show that the model scales well with the length of demonstrated action sequences, and that the majority of its memory usage during causal inference is dedicated to transient short-term memories, much like human working memory.

NeuroCERIL is distinguished from prior approaches to robotic imitation learning by its use of neural computations to understand demonstrated behavior in terms of causal relations that are directly related to high-level planning and cognitive-motor control. This not only affords generalization during imitation, but also facilitates an understanding of roles and perspectives that is critical to human-robot collaboration [7]. In addition, NeuroCERIL maintains a model of the external environment in memory and tracks changes that are induced by demonstrated motor activity. NeuroCERIL’s understanding of demonstrations therefore provides an awareness of the physical consequences of behavior that is critical for safe and effective deployment of robots in sensitive environments.

Causal reasoning and compositionality are widely considered to be critical components of human cognition that are challenging for contemporary neural models to learn [37, 38, 39, 40]. NeuroCERIL performs causal reasoning with compositional models in working memory that represent the external environment and encode high-level behavioral plans, and is therefore a significant step toward developing neural networks with human-like reasoning capabilities. In addition, we have previously proposed that neural models of working memory control, particularly in humanoid robots, provide a promising avenue to understanding conscious cognitive processing and its underlying basis in neural computations [18, 41]. NeuroCERIL is therefore also relevant to investigations of consciousness in machines and biological agents because it implements human-like cognitive algorithms in a brain-inspired neural architecture.

NeuroCERIL has several important limitations that suggest directions for future research. In this paper, we have focused on the causal inference component of imitation learning (left side of Figure 1), and have not addressed the generation of motor plans to implement learned skills during imitation. In prior work, we have shown that programmable neural networks can implement basic hierarchical planning, and can perform adaptable motor control in simulated robots [27, 30]. It is therefore feasible to integrate NeuroCERIL with low-level neural models of perception and motor control to create a complete neurocognitive imitation learning system that performs both causal inference and plan generation.

Our proposed hypothetico-deductive causal reasoning algorithm relies on constraints in demonstrated behavior. In particular, implementations of abstract intentions must be performed in a fixed order as specified in the causal knowledge-base, and cannot be broken up by unrelated actions. In reality, procedural tasks might involve interleaved action sequences performed with both hands, and may include steps that can be performed in arbitrary arrangements. Thus, future work might involve modifying our causal inference algorithm to support these variations. This might also permit generalization to additional cognitive domains in which hypothetico-deductive reasoning is relevant, such as visual scene understanding and linguistic processing.

Finally, NeuroCERIL uses a unified memory system that does not include functionally distinct short-term and long-term memory. This means that long-term memories such as programs and causal knowledge may be gradually degraded as new short-term memories are constructed during program evaluation. Our empirical results show that the majority of

memories constructed during causal inference are only accessed during a narrow window of time, and are therefore highly transient short-term memories. This suggests that NeuroCERIL would benefit from a functional separation of short-term and long-term memory to protect the latter from interference.

Acknowledgements

This work was supported by ONR award N00014-19-1-2044.

Data Availability

The datasets generated during and/or analysed during the current study are available in the NeuroCERIL repository, <https://github.com/vicariousgreg/neuroceril>

References

- [1] Susan S Jones. The development of imitation in infancy. *Philosophical Transactions of the Royal Society B: Biological Sciences*, 364(1528):2325–2335, 2009.
- [2] Andrew N Meltzoff, Patricia K Kuhl, Javier Movellan, and Terrence J Sejnowski. Foundations for a new science of learning. *Science*, 325(5938):284–288, 2009.
- [3] Harish Ravichandar, Athanasios S Polydoros, Sonia Chernova, and Aude Billard. Recent advances in robot learning from demonstration. *Annual Review of Control, Robotics, and Autonomous Systems*, 3:297–330, 2020.
- [4] Ahmed Hussein, Mohamed Medhat Gaber, Eyad Elyan, and Chrisina Jayne. Imitation learning: A survey of learning methods. *ACM Computing Surveys (CSUR)*, 50(2):1–35, 2017.
- [5] Aude Billard, Sylvain Calinon, Ruediger Dillmann, and Stefan Schaal. Survey: Robot programming by demonstration. Technical report, Springer, 2008.
- [6] Stefan Schaal. Is imitation learning the route to humanoid robots? *Trends in cognitive sciences*, 3(6):233–242, 1999.
- [7] J Gregory Trafton, Nicholas L Cassimatis, Magdalena D Bugajska, Derek P Brock, Farilee E Mintz, and Alan C Schultz. Enabling effective human-robot interaction using perspective-taking in robots. *IEEE Transactions on Systems, Man, and Cybernetics-Part A: Systems and Humans*, 35(4):460–470, 2005.
- [8] Garrett Katz, Di-Wei Huang, Theresa Hauge, Rodolphe Gentili, and James Reggia. A novel parsimonious cause-effect reasoning algorithm for robot imitation and plan recognition. *IEEE Transactions on Cognitive and Developmental Systems*, 10(2):177–193, 2017.
- [9] Gregory P Davis, Garrett E Katz, Rodolphe J Gentili, and James A Reggia. Neurolisp: High-level symbolic programming with attractor neural networks. *Neural Networks*, 146:200–219, 2022.
- [10] Albert Bandura. *Psychological modeling: Conflicting theories*. Transaction Publishers, New Jersey, USA, 2017.
- [11] Andrew N Meltzoff. Understanding the intentions of others: re-enactment of intended acts by 18-month-old children. *Developmental psychology*, 31(5):838, 1995.
- [12] Dare A Baldwin and Jodie A Baird. Discerning intentions in dynamic human action. *Trends in cognitive sciences*, 5(4):171–178, 2001.
- [13] Michael Tomasello, Ann Cale Kruger, and Hilary Horn Ratner. Cultural learning. *Behavioral and brain sciences*, 16(3):495–511, 1993.
- [14] Erhan Oztop, Mitsuo Kawato, and Michael A Arbib. Mirror neurons: functions, mechanisms and models. *Neuroscience letters*, 540:43–55, 2013.
- [15] Philip L Jackson, Andrew N Meltzoff, and Jean Decety. Neural circuits involved in imitation and perspective-taking. *Neuroimage*, 31(1):429–439, 2006.
- [16] Leonardo Fogassi, Pier Francesco Ferrari, Benno Gesierich, Stefano Rozzi, Fabian Chersi, and Giacomo Rizzolatti. Parietal lobe: from action organization to intention understanding. *Science*, 308(5722):662–667, 2005.
- [17] Moritz Köster, Miriam Langeloh, Christian Kliesch, Patricia Kanngiesser, and Stefanie Hoehl. Motor cortex activity during action observation predicts subsequent action imitation in human infants. *NeuroImage*, 218:116958, 2020.

- [18] James A Reggia, Garrett E Katz, and Gregory P Davis. Humanoid cognitive robots that learn by imitating: Implications for consciousness studies. *Frontiers in Robotics and AI*, 5:1, 2018.
- [19] Di-Wei Huang, Garrett Katz, Joshua Langsfeld, Rodolphe Gentili, and James Reggia. A virtual demonstrator environment for robot imitation learning. In *2015 IEEE International Conference on Technologies for Practical Robot Applications (TePRA)*, pages 1–6. IEEE, 2015.
- [20] Yan Duan, Marcin Andrychowicz, Bradly Stadie, Jonathan Ho, Jonas Schneider, Ilya Sutskever, Pieter Abbeel, and Wojciech Zaremba. One-shot imitation learning. In *Proceedings of the 31st International Conference on Neural Information Processing Systems*, pages 1087–1098, 2017.
- [21] YuXuan Liu, Abhishek Gupta, Pieter Abbeel, and Sergey Levine. Imitation from observation: Learning to imitate behaviors from raw video via context translation. In *2018 IEEE International Conference on Robotics and Automation (ICRA)*, pages 1118–1125. IEEE, 2018.
- [22] Danfei Xu, Suraj Nair, Yuke Zhu, Julian Gao, Animesh Garg, Li Fei-Fei, and Silvio Savarese. Neural task programming: Learning to generalize across hierarchical tasks. In *2018 IEEE International Conference on Robotics and Automation (ICRA)*, pages 3795–3802. IEEE, 2018.
- [23] Shao-Hua Sun, Hyeonwoo Noh, Sriram Somasundaram, and Joseph Lim. Neural program synthesis from diverse demonstration videos. In *International Conference on Machine Learning*, pages 4790–4799. PMLR, 2018.
- [24] Rudy Bunel, Matthew Hausknecht, Jacob Devlin, Rishabh Singh, and Pushmeet Kohli. Leveraging grammar and reinforcement learning for neural program synthesis. *arXiv preprint arXiv:1805.04276*, 2018.
- [25] David Silver, Aja Huang, Chris J Maddison, Arthur Guez, Laurent Sifre, George Van Den Driessche, Julian Schrittwieser, Ioannis Antonoglou, Veda Panneershelvam, Marc Lanctot, et al. Mastering the game of go with deep neural networks and tree search. *Nature*, 529(7587):484–489, 2016.
- [26] Ashwin Kalyan, Abhishek Mohta, Oleksandr Polozov, Dhruv Batra, Prateek Jain, and Sumit Gulwani. Neural-guided deductive search for real-time program synthesis from examples. *arXiv preprint arXiv:1804.01186*, 2018.
- [27] Gregory P. Davis, Garrett E. Katz, Rodolphe J. Gentili, and James A. Reggia. Compositional memory in attractor neural networks with one-step learning. *Neural Networks*, 138:78–97, 2021. ISSN 0893-6080.
- [28] Garrett E Katz, Gregory P Davis, Rodolphe J Gentili, and James A Reggia. A programmable neural virtual machine based on a fast store-erase learning rule. *Neural Networks*, 119:10–30, 2019.
- [29] Jared Sylvester and James Reggia. Engineering neural systems for high-level problem solving. *Neural Networks*, 79:37–52, 2016.
- [30] Garrett E Katz, . Akshay, Gregory P Davis, Rodolphe J Gentili, and James A Reggia. Tunable neural encoding of a symbolic robotic manipulation algorithm. *Frontiers in Neurorobotics*, page 167, 2021.
- [31] Rodolphe J Gentili, Hyuk Oh, Di-Wei Huang, Garrett E Katz, Ross H Miller, and James A Reggia. A neural architecture for performing actual and mentally simulated movements during self-intended and observed bimanual arm reaching movements. *International Journal of Social Robotics*, 7(3):371–392, 2015.
- [32] Anton E Lawson. How do humans acquire knowledge? and what does that imply about the nature of knowledge? *Science & Education*, 9(6):577–598, 2000.
- [33] Jan Sprenger. Hypothetico-deductive confirmation. *Philosophy Compass*, 6(7):497–508, 2011.
- [34] James A Marcum. An integrated model of clinical reasoning: dual-process theory of cognition and metacognition. *Journal of evaluation in clinical practice*, 18(5):954–961, 2012.
- [35] James A Reggia and Yun Peng. Modeling diagnostic reasoning: a summary of parsimonious covering theory. *Computer methods and programs in biomedicine*, 25(2):125–134, 1987.
- [36] Anton E Lawson. The generality of hypothetico-deductive reasoning: Making scientific thinking explicit. *The American Biology Teacher*, 62(7):482–495, 2000.
- [37] Brenden M Lake, Tomer D Ullman, Joshua B Tenenbaum, and Samuel J Gershman. Building machines that learn and think like people. *Behavioral and brain sciences*, 40, 2017.
- [38] Dieuwke Hupkes, Verna Dankers, Mathijs Mul, and Elia Bruni. Compositionality decomposed: How do neural networks generalise? *Journal of Artificial Intelligence Research*, 67:757–795, 2020.
- [39] Brenden Lake and Marco Baroni. Generalization without systematicity: On the compositional skills of sequence-to-sequence recurrent networks. In *International Conference on Machine Learning*, pages 2873–2882, 2018.

-
- [40] João Loula, Marco Baroni, and Brenden Lake. Rearranging the familiar: Testing compositional generalization in recurrent networks. In *Proceedings of the 2018 EMNLP Workshop BlackboxNLP: Analyzing and Interpreting Neural Networks for NLP*, pages 108–114, 2018.
 - [41] James A Reggia, Garrett E Katz, and Gregory P Davis. Modeling working memory to identify computational correlates of consciousness. *Open Philosophy*, 2(1):252–269, 2019.